ANALYSIS OF THE LEVEL OF OXIDATIVE PHOSPHORYLATION IN BREAST CANCER CELL TYPES

by

Bratislav M. Janjic

Diplom in Biology, Univerziteta u Beogradu, Yugoslavia, 1996

Submitted to the Graduate Faculty of

the Graduate School of Public Health in partial fulfillment

of the requirements for the degree of

Master of Science

University of Pittsburgh

2012

UNIVERSITY OF PITTSBURGH

GRADUATE SCHOOL OF PUBLIC HEALTH

This thesis was presented

by

Bratislav M. Janjic

It was defended on

April 6, 2012

and approved by

Thesis Advisor:
Ada Youk, PhD
Assistant Professor
Departments of Biostatistics and Epidemiology and Clinical & Translational Science
Graduate School of Public Health
University of Pittsburgh

Committee Member:
Bennett Van Houten, PhD
Professor
Departments of Pharmacology and Chemical Biology
University of Pittsburgh Cancer Institute
University of Pittsburgh

Committee Member:
Roger Day, ScD
Associate Professor
Department of Biomedical Informatics
School of Medicine
University of Pittsburgh

Ada Youk, PhD

ANALYSIS OF THE LEVEL OF OXIDATIVE PHOSPHORILATION IN BREAST CANCER CELL TYPES

Bratislav M. Janjic, MS

University of Pittsburgh, 2012

Aim. Glycolysis is a cell metabolic process by which glucose is converted to pyruvate. Under aerobic conditions, pyruvate is further oxidized by the citric acid cycle and oxidative phosphorylation (OXPHOS) to CO_2 and water. Under anaerobic conditions pyruvate is converted to lactate. Warburg first noted that cancer cells take up and metabolize glucose in excess of their bioenergetics and biosynthetic needs and produce more lactic acid in aerobic condition than normal cells. Our hypothesis was that cell lines originated from breast tumors have lower levels of oxidative phosphorylation compared to cell lines that originated from normal tissue. Moreover, we expected that tumor cell lines originated from highly aggressive tumors would have lower oxidative phosphorylation than the cell lines originated from less aggressive tumors and normal tissues.

Method. The change in cellular oxygen consumption rate (OCR) in the presence of pharmacological modulators is the most suitable measure of oxidative phosphorylation. The OCR was measured on basal-like, claudin-low, HER-2, luminal and normal cell types, each represented by different number of cell lines. OCR were measured first at base level and then after successive treatments with different pharmacological modulators. Basal OCR, total reserve capacity OCR and ATP-linked OCR were calculated for each cell line. The linear mixed effect

regression was used to define the model that described the best association between each of these dependent variables and the cell types, controlling for other variables.

Conclusion. We found that there is no significant difference in oxidative phosphorylation among basal-like, claudin-low and normal cell types. However, HER-2 and luminal cell types, originated from less aggressive tumors with better clinical outcome, did show statistically significant higher levels of oxidative phosphorylation than other types (basal-like, claudin-low).

Public health significance. It has been shown that breast cancer is the most common cancer among women of almost all races and it had been recognized as a major public health problem. Understanding metabolic differences between breast cancer cells and normal cells and among different type of breast cancer cells might have significance in designing appropriate chemo-therapeutics and treatment procedures for patients with different types of breast cancers.

TABLE OF CONTENTS

LIST OF TABLES

LIST OF FIGURES

1.0 INTRODUCTION

The most important catabolic reactions that generate free energy in any kind of eukaryotic cells are glycolysis and oxidative phosphorylation (OXPHOS). Glycolysis is the process that occurs in cytosol while oxidative phosphorylation occurs in mitochondrion. The released energy is conserved in the form of ATP and reduced coenzymes NADPH and $FADH_2$. These molecules are the major energy sources in the cell [1, 2].

During the process of glycolysis, a molecule of glucose is converted via fructose 1,6-bisphosphate to pyruvate. Under anaerobic conditions, pyruvate is converted to lactate, a reduced end product [1]. Under aerobic conditions pyruvate is further oxidized by the citric acid cycle and oxidative phosphorylation to CO_2 and water. This process occurs in mitochondrion [3, 4].

The mitochondrion is the site of eukaryotic oxidative metabolism, including citric acid cycle, electron transport and oxidative phosphorylation, fatty acid oxidation and amino acid breakdown. It contains all necessary enzymes that mediate these processes. Mitochondrial oxygen consumption reflects both the activities of the electron transport chain (ETC) and the tricarboxylate (TCA) cycle within mitochondria. The rate at which O_2 is consumed by mitochondria is a sensitive measure of the functioning of electron transport chain [5].

In normally differentiated cells, mitochondrial respiration uses pyruvate, fatty acids and amino acids to produce energy in the form of ATP through oxidative phosphorylation (OXPHOS). In this process protons are expelled from mitochondrion and the free energy stored in the resulting pH gradient drives the synthesis of ATP from ADP and Pi through electron transport chain (ETC). The process of complete oxidation of one molecules of glucose to CO_2

and H_2O generates a total of 10 molecules of reduced NADH and two molecules of reduced $FADH_2$. In the process of ETC, each molecule of NADH and $FADH_2$ generates about three and two molecules of ATP, respectively. Including two ATP generated in glycolysis in cytosol and two ATP generated in citric acid cycle, each molecule of glucose generates ~38 molecules of ATP [5-7]

In the sequence of electron transport in ETC, electrons are carried from NADH and $FADH_2$ to Complexes I and II, respectively and further to coenzyme Q (CoQ). From CoQ electrons are carried to complex III and from complex III to complex IV by the peripheral membrane protein cytochrome c. During the electron transport, H+ is pumped out the mitochondrial matric by complex I, III and IV, thereby generating an electrochemical gradient across the inner mitochondrial membrane. The exergonic return of these protons to the matrix powers the synthesis of ATP [8, 9].

Otto Warburg first described the high rate of glucose conversion to lactate in cancer cells compared to their normal cells, despite the presence of ample oxygen. This is well known as the Warburg effect [10, 11]. The altered cellular metabolism is a result of oncogenic transformation to a cancer phenotype [12, 13]. Genetic alterations in multiple signal pathways allow cancer cells to constitutively take up and metabolize glucose and glutamine in excess of their bioenergetics and biosynthetic needs [13-15]. Cellular oxygen consumption rate (OCR) was used to monitor oxidative phosphorylation in real time when appropriate pharmacological modulators were added to assay medium [16]. This parameter reflects qualitatively the rate of mitochondrial respiration. These studies demonstrated that some tumor cell lines displayed a dependency on glycolysis while their respiration was inhibited. The observed mitochondrial impairment was linked to the

increased dependency on glycolysis and might provide a mechanistic explanation for the growth advantage and apoptotic resistance of tumor cells [16].

In this study, OCR was measured in breast cancer tumor cell lines and normal cell lines, exposed to each of four well defined modulators of mitochondrial glycolytic energy metabolism (olygomicin, carbonyl cyanide p-[rifluorometoxyl]-phenyl-hydrazine (FCCP), 2-deoxyglycose (2-DG) and rotenone) using the XF24 Extracellular Flux Analyzer (Seahorse Biosciences, Bilerica, MA), a fully integrated 24-well instrument capable of measuring in real time the uptake and excretion of metabolic end products. (16).

Oligomycin, an antibiotic, acts by blocking ATP synthesis at complex V, causing proton build up on the outside of the inner mitochondrial membrane and loss of electron transport. This process is followed by decrease in oxygen consumption rate (OCR) [17]. Carbonyl cyanide p-trifluorometoxyl-phenyl-hydrazine (FCCP) is an uncoupler. It acts as an ionophore, completely dissipating the chemiosmotic gradient, uncoupling mitochondrial respiration from ATP synthesis leaving the electron transport system uninhibited. This invokes an increase in OCR [17]. Two-deoxyglucose (2-DG) is a glucose analog that inhibits hexokinase, the first enzyme glycolytic pathway, which converts glucose to glucose-6-phosphate, causing inhibition of glucose uptake. Addition of 2-DG after FCCP treatment causes an increase or no change in OCR[15]. Under this condition, fatty acids might be utilized as the major fuel for oxidative metabolism [17-19]. Finally, the addition of rotenone (an inhibitor of mitochondrial NADH dehydrogenase/complex I) completely blocks electron transport and OCR [16].

The aim of this study was to show that breast cancer cells have lower levels of oxidative phosphorylation than normal cells as a result of mitochondrial impairment in tumor cells. Within tumor cell lines, we wanted to show that tumor cells that are estrogen receptor positive (ER^+)

(luminal cell type), and human epidermal growth factor receptor 2 positive ($HER2^+$) (HER2 cell type) had higher levels of oxidative phosphorylation than triple negative (estrogen receptor negative (ER^-), progesterone receptor negative (PR^-) and $HER2^-$) (basal-like and claudin-low), which have worse clinical prognosis and further oncogenic transformation resulting in additional mitochondrial impairment [16, 20].

Based on OCR obtained over the treatment with metabolic modulators, the additional OCR measures (basal OCR, total reserve capacity and ATP-linked OCR) were calculated and used for better understanding bioenergetics differences between normal and tumor cell types and among different tumor cells types [16, 17]. Basal OCR was defined as the difference of the mean OCR of untreated cells and the mean OCR caused by non-mitochondrial respiration (OCR after the rotenone treatment) and represents the base level of oxidative phosphorylation of untreated cells. Total reserve capacity was defined as the difference of the mean of OCR after 2-deoxyglucose treatment and the mean OCR caused by non-mitochondrial respiration and represents the state where the cell approaches its maximum respiratory rate and depletes its reserve capacity. This parameter can be used as indicator how well the cell might deal with stress. ATP-linked OCR was defined as the difference of the mean basal level OCR and the mean of OCR after oligomycin treatment (caused by proton leak) and represents the respiration rate directly related to ATP synthesis [1, 17, 18].

2.0 STUDY METHODS

2.1 EXPERIMENTAL METHODS

Tumor cell lines used in the study were grouped into to four cell types, basal-like, claudin-low, luminal and HER-2, based on their clinical, pathological and biological features of the tumor type from which they were generated. Based on the expression of estrogen receptors (ER), progesterone receptor (PR) and epidermal growth factor receptor-2 (HER-2), the majority of triple-negative tumors, considered as the most aggressive, were either basal like or claudin-low, followed by HER-2 enriched and luminal [20].

The bioenergetic properties of four different tumor cells types (basal-like, claudin-low, luminal and Her-2) and one normal cell type were analyzed after the treatment with different metabolic modulators. Basal-like tumor cell type was represented by two cell lines (BT-20 and HCC1143), claudin-low by four tumor cell lines (BT549, MDA-MB 231, MDA-MB 157 and Hs578T), luminal by five tumor cell lines (MCF7, BT474, ZR 75 1, CAMA-1 and MDA-MB 361), HER-2 cell type by two tumor cell lines (MDA-MB 453 and SK-BR 3) and normal cell type by four cell lines (HMEC, BRL36, BRL11 and BRL23).

The cells were seeded in XF 24-well cell culture microplates (Seahorse, Bioscience) at 40,000 cells/well in 500 ul growth media and incubated at 37^{o}C, 5% CO_2 for 20-24h. After the baseline measurement, the testing agent was prepared in assay medium that was injected into

each well to reach the desired final working concentration and the oxygen consumption rate (OCR) was measured. Multiple measurements as well as compound injections were made at the indicated time points by the following procedure: after estimating the basal level of OCR on untreated cells, oligomycin, FCCP, 2-DG and rotenone were sequentially injected through ports to final concentrations of 1uM, 300nM, 100mM and 1uM, respectively. Four baseline rates and three response rates for each metabolic modulator were measured, for a total of 16 measurements during the time 0-132 minutes. At the end of each assay, cells were detached by incubating with 0.25% trypsin (Invitrogen), and the number and percentage of viable cells was determined by Trypan blue exclusion assay. The OCR level was normalized to the same number of cells and expressed as pMoles/min/10^3 cells [15]. For each cell type, basal OCR, total reserve capacity and ATP-linked OCR values were calculated.

2.2 LINEAR MIXED EFFECT MODELS

Linear mixed effect modeling is an approach for analyzing longitudinal data. In linear mixed effect models the mean response is a combination of population characteristics, named fixed effects, shared by all individuals and subject-specific effects, named random effects, unique to a particular individual. The term mixed denotes the presence of both fixed and random effects in a single model [21].

These models allow the analysis of between-subject and within-subject source of variability in the longitudinal response. Using this model, it is possible to describe not only how the mean responses changes in the population of interest, but also how individual response change over time.

In general form, linear mixed effect model can be expressed, using vector and matrix notation, as:

$$Y_i = X_i \beta + Z_i b_i + e_i$$

Where i represents the subject number, β is a (p x 1) vector of fixed effect, b_i is a (q x 1) vector of random effects, X_i is a (n_i x p) matric of covariates and Z_i is a (n_i x q) matrix of covariates, with $q \leq p$

In this case, the conditional or subject specific mean for given bi in this case would be:

$$E(Y_i|b_i) = X_i \beta + Z_i b_i$$

while the marginal or population-averaged mean of Y_i, averaged over the random effect b_i, would be:

$$E(Y_i) = X_i \beta, \text{ since } E(b_i)=0$$

The regression parameters β are the same for all individuals, while b_i, combined with the corresponding fixed effects, are subject specific regression coefficients.

In the simplest linear mixed effect model, it has been assumed that intercept randomly varies from one individual to another and the model can be presented as following:

$$E(Y_{ij}) = X_{ij}\beta_j + b_i + e_{ij}$$

where X_{ij} are covariates, β's are regression parameters, b_i is the random subject effect and e_{ij} are the sampling errors. The models describes the difference of the response for the i^{th} subject at the j^{th} measuring occasion from the population mean, $X_{ij}\beta_j$, by a subject effect bi, within-subject measurement error, e_{ij} [23]. Both the subject effect and the residual variation are assumed to be random, with mean zero and variance $Var(b_i) = \sigma_b^2$ and $Var(e_{ij})=\sigma^2$. Based on this, the model describes the conditional mean response of Y_{ij} for any individual, with the given subject-specific effect:

$$E(Y_{ij}|b_i) = X_{ij}\beta + b_i$$

The marginal mean of Y_{ij}, averaged over the distribution of the subject-specific effect, b_i, is given by:

$$E(Y_{ij}) = X_{ij}\beta$$

In this model the regression parameter β describes the change of the response over time in the population, while b_i describes how the trend of i^{th} individual deviates from the population's intercept after accounting for the effect of covariates [21, 22].

In case when intercepts and slopes vary randomly among individuals, a linear effect model for i^{th} subjects and j^{th} measurements is given by:

$$Y_{ij} = \beta_0 + \beta_1 t_{ij} + b_{0i} + b_{1i}t_{ij} + e_{ij}, j=1,\ldots, ni,$$

where β_0 and β_1 are population regression parameters, while b_{0i} and b_{1i} are random effect regression parameters.

After making the assumption that the response vector *Yi* arose from a multivariate normal distribution with the covariance matrix $Cov(Y_i) = \Sigma i = \Sigma i(\theta)$, we use maximum likelihood estimate (MLE) as a general estimation approach for the estimate of β and θ values, which estimates these values as most likely for the observed data [23].

To test the significance of regression parameters and significance of the difference between levels of the main effect categorical variable, the likelihood ratio test (LRT) and Wald test were used, respectively. It has been shown that the *-2log* ratio between the likelihood function over the null hypothesis and the likelihood function over the model follows a Chi-square distribution with the degrees-of-freedom (df) equal to the difference in the number of parameters in the model and null hypothesis [21]. The Wald test is an approximation of likelihood ratio test and is defined as the squared ratio between an estimate and its corresponding standard deviation:

$$W=(estimate/\ SD(estimate))^2$$

In the situation where the central limit theorem (CLT) applies, the estimate will have an approximate normal distribution and, therefore, the quantity of Wald statistics will have approximately Chi-square distribution with one degree of freedom and thus large values will lead to a rejection of the null hypothesis. If the test statistics fails to reject the null hypothesis, removing the variables from the model will not substantially harm the fit of that model [21, 24].

2.3 STATISTICAL ANALYSIS

Descriptive statistics were computed to show the distribution and potential outliers of oxygen consumption rate (OCR) which is the dependent variable in the mixed models. OCR was analyzed over the lines (CLINE), cell types (CTYPE), and experiment number (EXPDATE).

We compared oxygen consumption rate among different cell types (CTYPE) using linear mixed effect models, with a random effects for each well of 24 well plates seeded with cells of the specific cell line used in experiments. This model was fit controlling for treatment (TREATM), cell lines (CLINE), experiment number (EXPDATE) and time (TIME). Possible interactions of statistically significant variables were assessed. All independent variables (treatment, cell line, experiment number, and time) were treated as fixed effect variables, where the treatment variable represented the untreated and 4 levels of successive treatments with different metabolic modulators (oligomycin, FCCP, 2-DG and rotenone) and cell line (CLINE) variable represented 17 different cell lines used in the study, belonging to five different cell types (CTYPE). Experiment number (DATAEXP) represented the experiment number variable with 15 levels, where each level is the set of experiments involving different cell lines coming from different cell types, performed at the same day. Time (TIME) was a variable with 16 levels, which represented the period from 0 to 132 minutes when the measures of OCR were taken.

First, a univariate analysis of each separate variable was performed. Variables were kept in the multivariate model if statistically significant at $p<0.05$ in the univariate analysis. After establishing the appropriate multivariable regression model, model diagnostics were performed by checking for heteroscedasticity and departure from normality of the dependent variable using scatter plots of combined fixed and random effect residuals over the predicted values of OCR,

standardized normal probability plots, quantile plots and univariate kernel density plots of the residuals.

Basal OCR, total reserve capacity and ATP-linked OCR were calculated for each cell line used in the study. Descriptive statistics for each of these OCR measures were calculated over cell type (CTYPE). Linear mixed effect models was fit to assess differences in basal OCR, total reserve capacity and ATP-linked OCR between the cell types (CTYPE), using cell line (CLINE) and experiment number (EXPDATE) as a random effects. Model diagnostics were performed on the final models. P values < 0.05 were defined as statistically significant.

Data analyses were performed using MS Excel 2010 (Microsoft, Redmond, WA) and Stata SE/12 (StataCorp LP, College Station, TX).

3.0 RESULTS

As shown in Table 1, oxygen consumption rate (OCR) was measured for normal and tumor cell types, represented by total of 17 cell lines. Different number of replicates was used for each of the cell lines. Over the time period from 0-132 minutes, 16 successive measures of OCR were taken: four on untreated cells after 1, 10, 19 and 28 minutes of incubation, three measures on oligomycin treated cells after 36, 45, and 54 minutes, three measures for FCCP treated cells, after 64, 73 and 82 minutes, three measures for 2-DG treatment, after 91, 99 and 108 minutes and three measures after rotenone treatment, at 115, 124 and 132 minutes of incubation. The experiments were repeated from two to five times and the number of replicates for each cell line per experiment was in the range from two to seven (Tables 1 and 2). Basal-like cell type was represented by two cell lines BT20 and HCC1143 (17.04%), Claudine-low was represented by four cell lines BT549, Hs578T, MDA-MB 157 and MDA-MB 231 (22.73%), Luminal cell type was represented by five cell lines, MCF-7, MT474, ZR-75, CAMA-1 and MDA-MB 361 (30.68%), (Table 1). Oxygen consumption rate was measured for each cell line separately at different treatment levels (without treatment and oligomycin, FCCP, 2-DG and rotenone treatment). The mean, standard deviation of OCR were calculated for each cell type (CTYPE), as given in table 3.

The base level of OCR for untreated cells had a mean range from 3.079 pmol/min/10^3 cells for claudin-low cell lines to 7.626 pmol/min/10^3 cells for luminal cell lines. Oligomycin

treatment decreased the OCR in all cell lines from 1.182 pmol/min/10^3 cells for basal-like to 2.701 pmol/min/10^3 cells for luminal cell lines. After FCCP treatment, the range of OCR was 4.277 pmol/min/10^3 cells for basal-like cell lines to 13.259 pmol/min/10^3 cells for luminal cell lines while subsequent treatment with 2-DG reduced the OCR down from 5.129 pmol/min/10^3 cells for basal-like cell lines to 15.205 pmol/min/10^3 cells for luminal cell lines. Finally, rotenone treatment dropped the OCR from 0.836 pmol/min/10^3 cells for basal-like cell lines to 2.284 pmol/min/10^3 cells for luminal cell lines (Table 3).

Summary statistics for the OCR values over 17 analyzed cell lines, five cell types, treatments and experiment number are presented in figures 1, 2 and 3, respectively. Figure 1 showed the distribution and outliers of OCR over analyzed cell lines. It can be observed higher interquartile range in luminal tumor cells lines (ZR 75 1, MDA-MB 361 and SKBR-3 compared to all other cells lines.

As seen in figure 2, there were a large number of outliers for OCR in the luminal cell type. Figure 3 showed that experiment number 4 had the highest interquartile range and the most outliers compared to all other experiments.

The difference in means and standard deviations among different cell types, untreated and treated with metabolic modulators are shown in table 3. As shown, luminal and HER-2 cell types had higher oxygen consumption rates than basal-like, claudin-low and normal cell types in all treatment conditions.

Linear mixed effect model was used to assess the association between the OCR and the cell types (CTYPE) as the main effect variable, having the experiment number (EXPDATE) as control variable (Table 4). There was no statistically significant interaction between the cell type and experiment number variables. Model diagnostics based on scatter plot of combined fixed and

random effect residuals over fitted values of OCR, normal and quantiles of residuals and a kernel density plot of the residuals showed small deviation from normality (Figure 4).

Wald test statistics showed statistically significant differences in OCR levels between normal and luminal tumor cell types ($p<0.00001$), normal and HER-2 ($p<0.00001$), basal-like and luminal cell types ($p<0.00001$), basal-like and HER-2 ($p<0.00001$), claudin-low and luminal ($p<0.00001$), claudin-low and HER-2 cell lines ($p<0.00001$) and luminal and HER-2 cell types ($p<0.00001$) (Table 5).

The descriptive statistics for basal OCR, total reserve capacity and ATP-linked OCR are shown in table 6. The range of values for basal OCR went from 2.112 pMol/min/10^3 for claudin-low cell lines to 5.341 pMol/min/10^3 for luminal cell type. total reserve capacity range had values from 4.293 to 12.920 pMol/min/10^3 for luminal cell lines, while ATP-linked OCR had a range from 2.722 to 7.210 pMol/min/10^3 for luminal cell lines. The distribution and outliers of basal OCR, total reserve capacity and ATP-linked OCR over the cell types are shown in figure 5. As shown, luminal and Her-2 tumor cell types showed the highest levels of basal OCR, total reserve capacity and ATP-linked OCR, while their levels are similar among basal-like, claudin-low and normal cell types. Luminal cell type showed higher variation of dependent variable in all three OCR measures and higher number of outliers than other analyzed cell types.

The linear mixed effect models for basal OCR, total reserve capacity and ATP-linked OCR included “cell type” as the main effect variable and the “experiment number” as the control variable. There was no statistically significant interaction between these two independent variables in either model. The regression parameter estimates and corresponding standard errors and p-value are shown in table 7. The model diagnostics for each of these three models, using

scatter plots of residuals versus fitted values, normal probability and quantiles of residuals and kernel density plots showed no significant departure from normality (Figure 6).

Statistically significant differences for basal OCR were found between normal and luminal cell types ($p<0.00001$), normal and HER-2 cell types ($p=0.051$), basal-like and luminal ($p<0.00001$), basal-like and HER-2 ($p=0.0112$), claudin-low and luminal ($p<0.00001$), claudin-low and HER-2 ($p=0.0030$) and luminal and HER-2 ($p=0.0001$). Statistically significant differences for total reserve capacity were found between normal and luminal cell types ($p=0.0010$), basal-like and luminal cell types ($p<0.00001$), basal-like and HER-2 ($p<0.0467$), claudin-low and luminal ($p<0.00001$), claudin-low and HER-2 ($p=0.0301$), luminal and HER-2 ($p=0.0044$). Statistically significant differences for ATP-linked OCR were found between normal and luminal cell types ($p=0.0002$), basal-like and luminal ($p=0.0001$), claudin-low and luminal ($p<0.00001$), luminal and HER-2 ($p<0.0010$) (Table 8).

4.0 DISCUSSION

Otto Warburg (1956) postulated that cancer cells, compared to normal cells, have an increased rate of glycolysis and decreased oxidative phosphorylation due to impairment of mitochondrial respiration, [10]. In this study we investigated the bioenergetics profile of four breast cancer cell types (basal-like, claudin-low, luminal and HER-2) classified by their gene profile and clinical outcome [19]. We compared the level of oxidative phosphorylation of tumor and normal cell lines by measuring oxygen consumption rates during the treatment with metabolic modulators, using XF24 Extracellular Flux Analyzer. This is a non-destructive method that does not require cell destruction and mitochondria isolation. It enables the analysis of the cell oxidative phosphorylation under physiological conditions [25]. We postulated that tumor cells originated from breast tumors have lower oxidative phosphorylation than normal cells. We also postulated that tumor cells originated from triple negative (ER^-, PR^- and $HER\text{-}2^-$) tumors have lower level of oxidative phosphorylation then tumor cells originated from clinically less aggressive tumors due to advanced stage of mitochondrial impairment caused by advanced stage of oncogenic transformation.

OCR of normal and tumor cells lines was measured in 15 experiments. The frequency of tumor cell lines and tumor cell types and number of repetitions in each experiment was heterogenic in order to prevent random error, as observed in table 1 and table 2. The mean OCR was calculated for each treatment condition and plotted over the experiment number. As shown,

the highest number of outliers was present in experiment 4, while the distribution of OCR over all other experiments was homogeneous (Figure 3). Plotting OCR over cell lines showed that cell lines from luminal cell type have higher interquartile range compared to all other cell lines (Figure 1) with the extreme values of ZR-75 1 cell line (Figure 1). Twelve out of 21 observations in experiment 4 were from luminal cell type and 6 out of these 12 observations were made on ZR-75 1 cell line (Table 2). This excluded random error as a source of variation and high number of outliers.

Comparing OCR between tumor and normal cell types, we found that normal cells did not have significantly higher oxidative phosphorylation than tumor cells (Figure 1). Moreover, analyzed normal cell lines showed similar or lower level of oxidative phosphorylation than most of tumor cell lines (Figure 2). Using linear mixed effect model and Wald test we showed that there were no significant differences in oxidative phosphorylation levels among normal, basal-like and claudin-low cell types. Luminal and HER-2 cell types showed significantly higher OCR than normal cell type. These findings were opposite to published data claiming that tumor cells have lower level of oxidative phosphorylation than normal cells [10].

Our findings indicated that tumor cell types represented by cell lines generated from triple negative (ER^-, PR^-, $HER\text{-}2^-$) tumors with worse clinical prognosis (basal-like and claudin-low) showed significantly lower level of oxidative phosphorylation than cell lines generated from tumors with clinically better prognosis (luminal, HER-2), which correspond to our assumption (Figure 2, Table 3).

Additional measures of oxygen consumption rate (basal OCR, total residual capacity and ATP-linked OCR) showed similar trend among analyzed cell types. Basal OCR is a measure of oxidative phosphorylation at the base level, without any treatment. There were no significant

differences in the level of oxidative phosphorylation among normal, basal-like and claudin-low cell types [Figure 5, Table 6]. Luminal and HER-2 cell type showed significantly higher oxidative phosphorylation level than basal-like, claudin-low and normal cell types. Total reserve capacity is a measure of maximum respiratory rate of the cell. There were no significant differences in total residual capacity among basal like, claudin-low and normal cell types. Luminal and HER-2 cell types showed significantly higher total reserve capacity from basal-like and claudin-low cell line, while no statistically significant difference between HER-2 and normal cell type. ATP-linked OCR was a measure of oxygen consumption rate directly linked to ATP synthesis in electron transport chain (ETC). It was proposed that tumor cells would have lower OCR due to lower mitochondrial respiration. We showed that there were no statistically significant differences in ATP-linked OCR among basal-like, claudin-low and normal cell types.

As shown in table 1 the number of experimental replicates per cell line varies from nine (BRL11) to 30 for (MCF-7). In most of the experiments MCF-7 has been used as a control cell line in the study, to monitor the consistency of the experimental conditions and the measuring equipment performance. MCF-7 cell line showed some variability in OCR values, but this seems rather the property of luminal cell type than problem with the experimental conditions and measuring equipment (figure 1). A total of 15 experiments were performed and number of different cell types analyzed per each experiment was from one (experiment 14 and 15, when only cell lines from normal cell types were used) to five (experiment 3, when the cell lines from all five cell types were analyzed) (Table 2). To avoid potential random error it would be preferable to run more than one cell type per experiment and at least one cell type with already know bioenergetics profile through the whole set of experiments, especially cell type of significant interest for was used (normal cell type).

To account for possible variability among different experiments, the "experiment number" variable was used as random effect and control variable in each model.

Although the interaction was not statistically significant, we assess its effect by comparing all models with and without the interaction parameter in, trying to address the possible differences among experiments. The results from these analyses were similar in terms of variance and normality of residuals and comparison of OCR measures between pairs of cell types.

As shown in table 2, normal and tumor cell types were paired in the experiments 2, 3 and 5, while in the experiments 14 and 15 only normal cell types were assessed, without using any cell line of known bioenergetics profile as control. This might prevent detection of possible random error in these two experiments. To address possible error, a model without data from experiment 14 and 15 should be compared with the full model, containing all data points. This comparison was not performed because triplicates of only one cell line (HMEC) were used in experiments 2, 3 and 5, while all other normal cell lines were included in experiments 14 and 15.

As shown in table 8, no statistically significant differences in ATP-linked OCR were found between HER-2 and basal-like, HER-2 and claudin-low, and HER-2 and normal cell types while the differences among these three pairs of cell types were obvious (figure 5). The reason for not being able to show the significant statistical difference ($p<0.05$) might be low power of the test statistics due to low sample number, since both basal-like and HER-2 cell types were represented by two cell lines each. Adding more additional cell lines would probably improve the power of the statistical analysis.

5.0 CONCLUSION

Analysed breast cancer tumor cell types (basal-like, claudin-low, luminal and HER-2) did not show lower level of oxidative phosphorylation than normal cell types. Within analysed tumor cell types, tumor cells originated from more aggressive, triple negative (ER^-, PR^- and $HER\text{-}2^-$) tumors (basal-like and claudin-low) showed significantly lower level of oxidative phosphorylation than tumor cells originated from less aggressive tumors (luminal and HER-2).

APPENDIX A: FIGURES AND TABLES

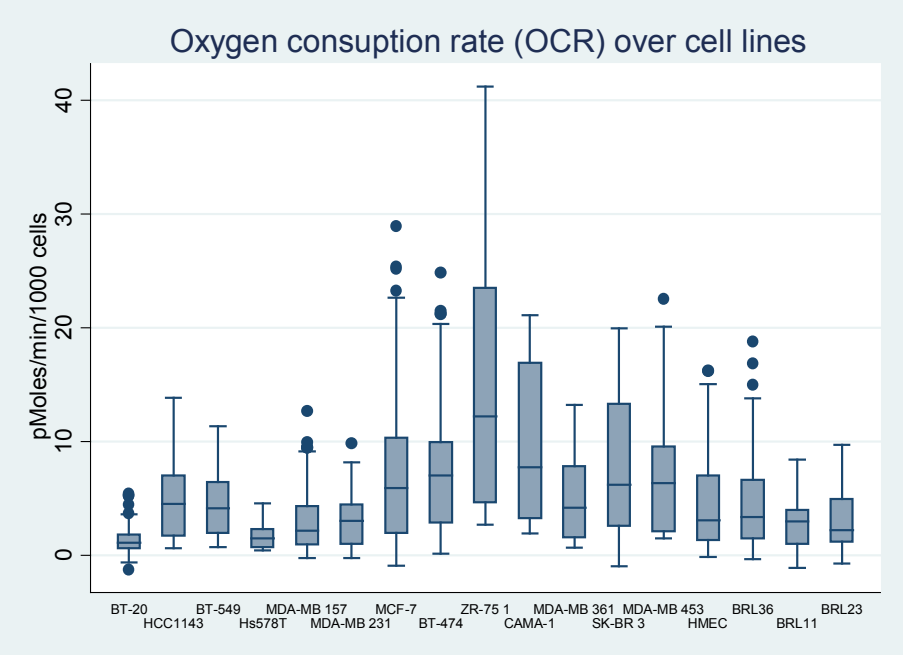

Figure 1. Box plot of oxygen consumption rate (OCR) over cell lines. Interquartile range, median, minimum, maximum, outliers and overall distribution of data points are shown for each cell line.

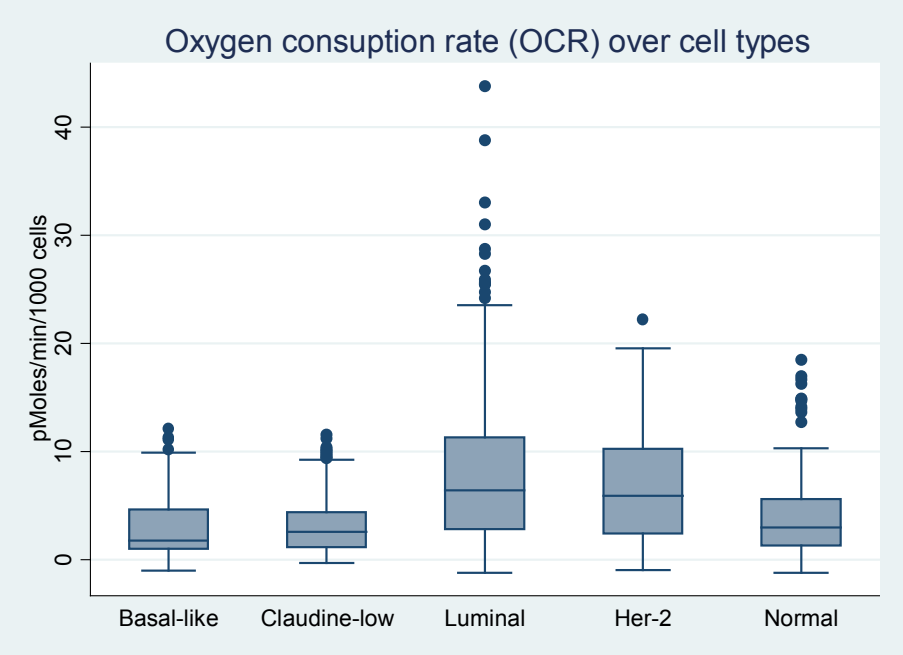

Figure 2. Box plot of oxygen consumption rate (OCR) of basal-like, claudin-low, luminal, HER-2 and normal cell types. Observed outliers in luminal cell type originated from ZR 75 1 cell line.

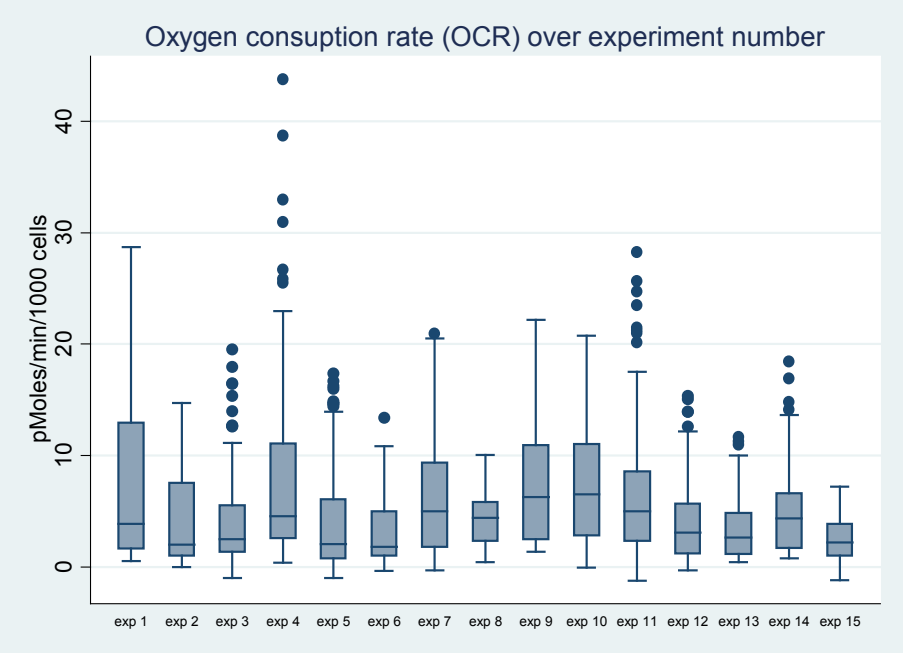

Figure 3. Box plot of oxygen consumption rate over experiment number. High number of outlier in experiment 4 originated from ZR 75 1 tumor cell line that showed the highest OCR among analyzed cell lines.

Table 1. The number of replicates of cell lines in the study. MCF-7 tumor cell line has the highest number of replicates (30, 11.36%) since it was used as internal control to monitor the consistency of experimental conditions and instrument performance.

	Cell lines	Total (%)
Basal-like	BT-20	23 (8.71%)
	HCC1143	22 (8.33%)
Claudin-low	BT-549	12 (4.55%)
	Hs578T	9 (3.41%)
	MDA-MB 157	16 (6.06%)
	MDA-MB 231	23 (8.71%)
Luminal	MCF-7	30 (11.36%)
	BT-474	21 (7.95%)
	ZR-75 1	9 (3.41%)
	CAMA-1	12 (4.55%)
	MDA-MB 361	9 (3.41%)
Her-2	SK-BR 3	21 (7.95%)
	MDA-MB 453	12 (4.55%)
Normal	HMEC	9 (3.41%)
	BRL36	14 (5.30%)
	BRL11	8 (3.03%)
	BRL23	14 (5.30%)
	Total	264 (100.00%)

Table 2. The frequency and percentage of cell types per experiment. Different cell types were used in each experiment to prevent random error due to potential variations in experimental conditions among different experiments.

	Basal-like	Claudin-low	Luminal	Her-2	Normal	Total
Exp 1		3 5.00%	3 3.70%	3 9.09%		9 3.41%
Exp 2	3 6.67%		6 7.41%		3 6.67%	12 4.55%
Exp 3	3 6.67%	3 5.00%	6 7.41%	3 9.09%	3 6.67%	18 6.82%
Exp 4	3 6.67%	3 5.00%	12 14.81%	3 9.09%		21 7.95%
Exp 5	7 15.56%	5 8.33%	7 8.64%		3 6.67%	22 8.33%
Exp 6	7 15.56%	5 8.33%	7 8.64%			19 7.20%
Exp 7	6 13.33%	6 10.00%	6 7.41%			18 6.82%
Exp 8	6 13.33%	6 10.00%	6 7.41%			18 6.82%
Exp 9			6 7.41%	12 36.36%		18 6.82%
Exp 10			6 7.41%	12 36.36%		18 6.82%
Exp 11	5 11.11%	11 18.33%	6 7.41%			22 8.33%
Exp 12	5 11.11%	9 15.00%	5 6.17%			19 7.20%
Exp 13		9 15.00%	5 6.17%			14 5.30%
Exp 14					16 35.56%	16 6.06%
Exp 15					20 44.44%	20 7.58%
Total	45 100%	60 100%	81 100%	33 100%	45 100%	264 100%

Table 3. Means and standard deviations (sd) of oxygen consumption rate (OCR) over the cell types for different treatment conditions. untreated, oligomycin, FCCP, 2-DG and rotenone treated.

OCR	Treatment									
	Untreated		Oligomycin		FCCP		2-DG		Rotenone	
Cell types	mean	sd	Mean	sd	mean	sd	mean	sd	mean	sd
Basal-like	3.233	1.928	1.182	0.747	4.277	3.174	5.129	2.883	0.836	0.659
Claudin-low	3.079	1.290	1.325	0.711	4.828	2.437	5.728	2.540	0.967	0.593
Luminal	7.626	3.404	2.701	1.426	13.259	6.110	15.205	7.117	2.284	1.439
Her-2	6.383	1.326	2.485	0.664	10.797	2.827	12.944	3.689	1.710	0.736
Normal	3.509	1.623	1.197	0.736	6.456	3.481	7.208	3.959	1.127	0.806

Table 4. Regression parameter estimates, standard errors and p-values using linear mixed effect model. The main effect variable "cell type" was treated as categorical variable. "Normal" cell type was omitted in the model and used as reference class.

	Oxygen consumption rate (OCR)		
Independent variable	**Estimate**	**Standard error**	**P-value**
Basal-like	-0.908	0.560	0.105
Claudin-low	-0.673	0.503	0.181
Luminal	4.376	0.506	<0.0001
Her2	3.016	0.589	<0.0001
Experiment number	0.011	0.041	0.790
Variances of random effect variables and residuals			
Subject	0.832		
Experiment number	0.831		
Residuals	21.160		

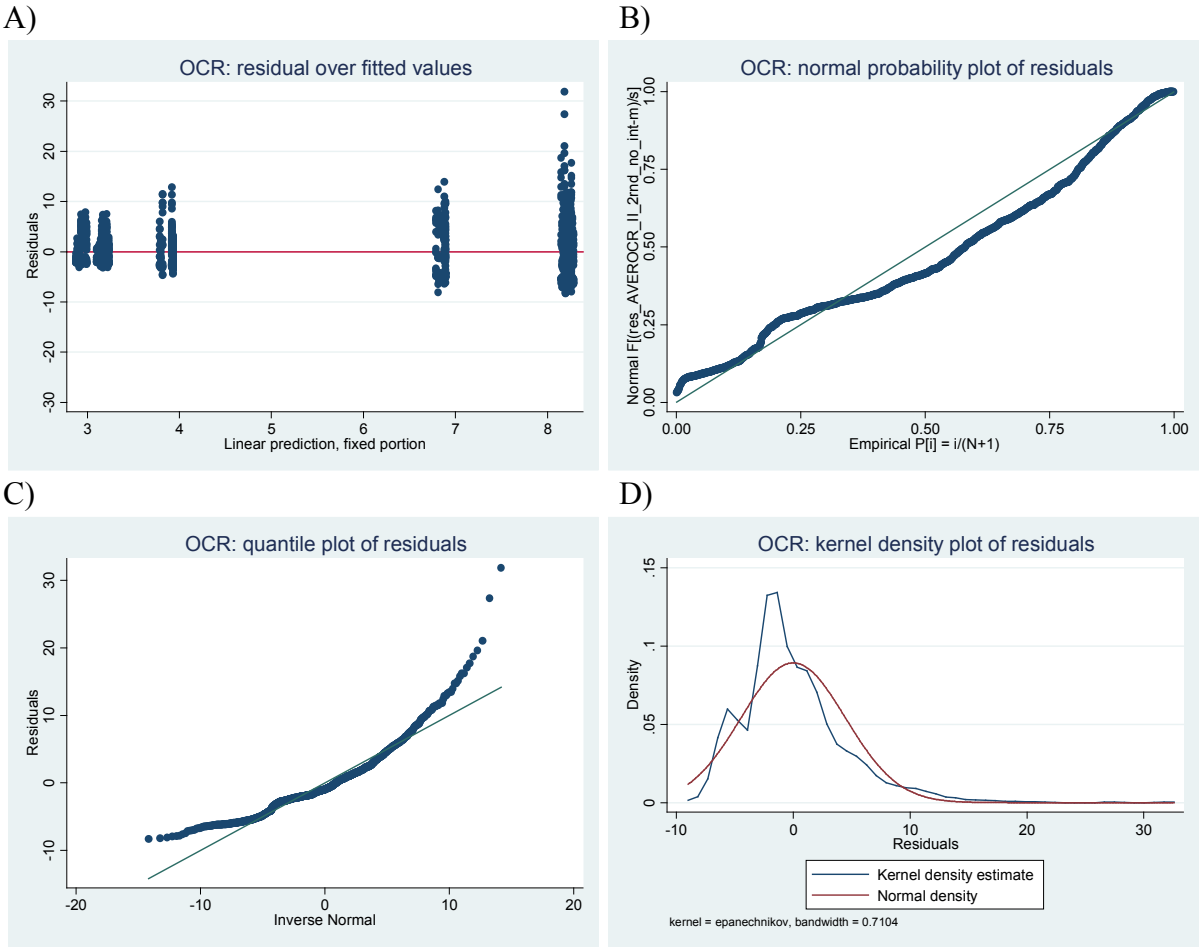

Figure 4. Linear mixed effect model diagnostic plots. A) Scatter plot of residuals over fitted values, B) Standardized normal probability plot of residuals, C) Quantile plot of residuals, D) Kernel density plot of residuals over normal distribution. The residuals showed small deviation from normality, but not enough to declare non-normality.

Table 5. Comparison of oxygen consumption rate (OCR) between pairs of analyzed cell types using Wald test on linear mixed effect model.

Cell type comparison			OCR (p-value)
Normal	vs.	Basal-like	0.1048
Normal	vs.	Claudin-low	0.1813
Normal	vs.	Luminal	<0.00001*
Normal	vs.	Her-2	<0.00001*
Basal-like	vs.	Claudin-low	0.2401
Basal-like	vs.	Luminal	<0.00001*
Basal-like	vs.	Her-2	<0.00001*
Claudin-low	vs.	Luminal	<0.00001*
Claudin-low	vs.	Her-2	<0.00001*
Luminal	vs.	Her-2	<0.00001*

* statistically significant values at the significance level $p<0.05$

A)

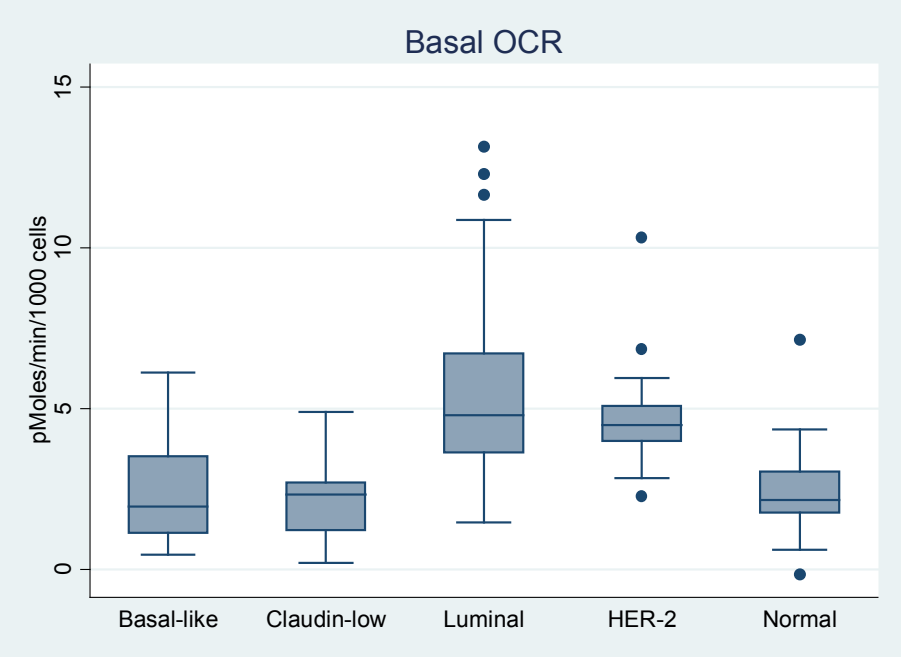
Basal OCR
pMoles/min/1000 cells
0
5
10
15
Basal-like
Claudin-low
Luminal
HER-2
Normal

B)

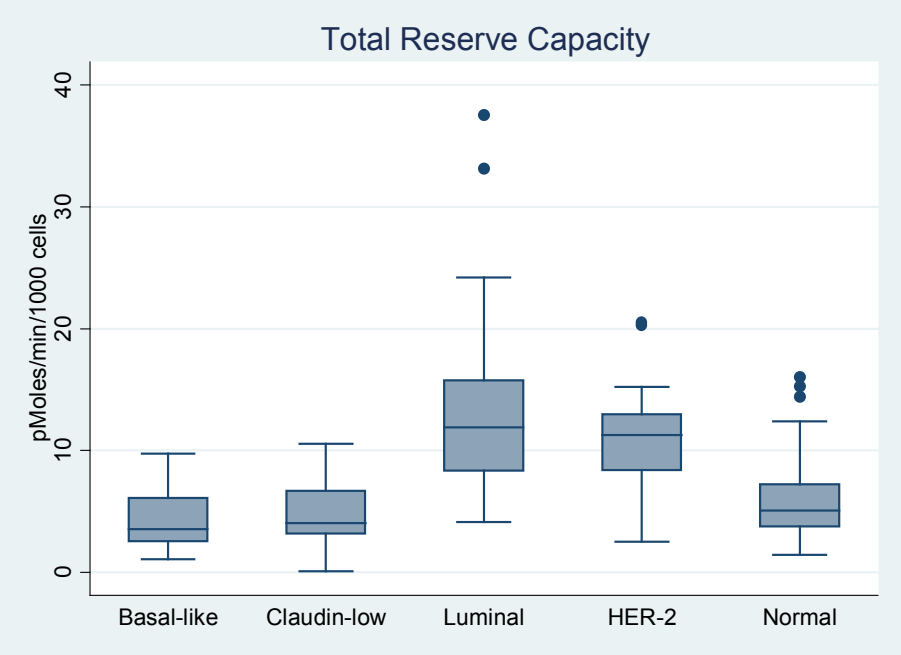
Total Reserve Capacity
pMoles/min/1000 cells
0
10
20
30
40
Basal-like
Claudin-low
Luminal
HER-2
Normal

C)

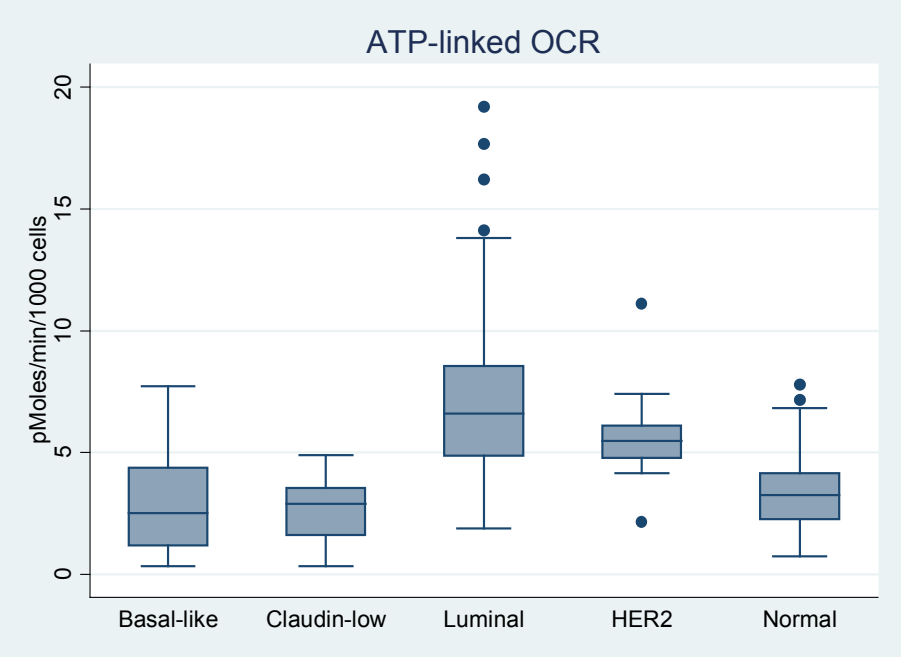

Figure 5. Box plots of basal OCR A) total reserve capacity B) and ATP-linked OCR C), over the cell types. Oxygen consumption rates were normalized per 1000 cells.

Table 6. Means and standard deviation (sd) of basal OCR, total reserve capacity and ATP-linked OCR by cell types.

	OCR measures					
	Basal OCR		**Total reserve Capacity**		**ATP-linked OCR**	
Cell types	**Mean**	**SD**	**Mean**	**SD**	**Mean**	**SD**
Basal-like	2.397	1.347	4.293	2.334	2.886	1.839
Claudin-low	2.112	0.959	4.761	2.265	2.722	1.165
Luminal	5.341	2.461	12.920	6.106	7.210	3.365
Her-2	4.673	1.363	11.234	3.711	5.608	1.408
Normal	2.382	1.206	6.081	3.470	3.439	1.709

Table 7. Regression parameter estimates, standard errors (se) and p-values (p), variance of random effect variables and residuals, using linear mixed effect model for basal OCR, total reserve capacity and ATP linked OCR. "Normal" cell type was omitted in the model and used as a reference class. "Cell line" and "experiment number" were used as random effect variables.

	Basal OCR			**Total reserve capacity**			**ATP-linked OCR**		
	Estimate	**SE**	**p**	**Estimate**	**SE**	**p**	**Estimate**	**SE**	**p**
Basal-like	0.216	0.882	0.806	-0.2398	2.453	0.328	-0.199	1.482	0.893
Claudin-low	-0.267	0.758	0.724	-2.146	2.076	0.301	-0.612	1.240	0.621
Luminal	3.152	0.756	<0.0001	6.768	2.057	0.001	4.541	1.219	<0.0001
Her-2	2.558	0.914	0.005	4.221	2.511	0.093	2.592	1.504	0.085
Expnum.	0.054	0.052	0.302	-0.108	0.130	0.405	0.069	0.069	0.315
Variances of random effect variables ("cell line" and "experiment number") and residuals									
Cell line	0.522			5.299			2.247		
Expnum.	1.237			5.904			1.374		
Residuals	0.986			6.617			1.783		

I) Basal OCR

A)

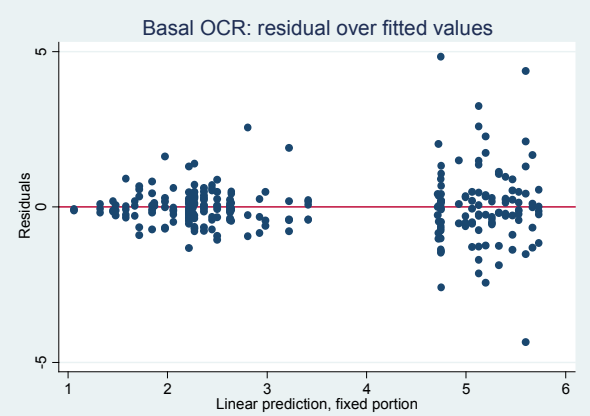

B)

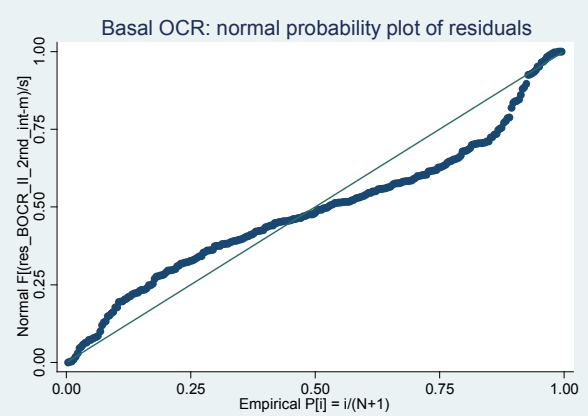

C)

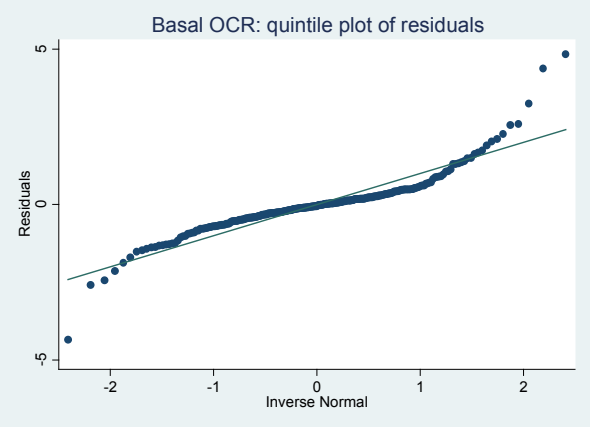

D)

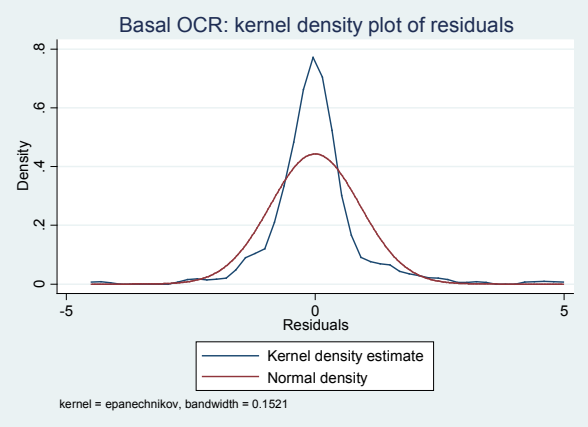

II) Total Reserve Capacity

A)

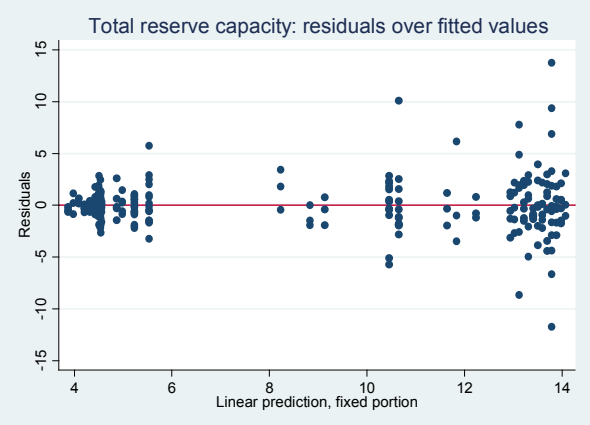

B)

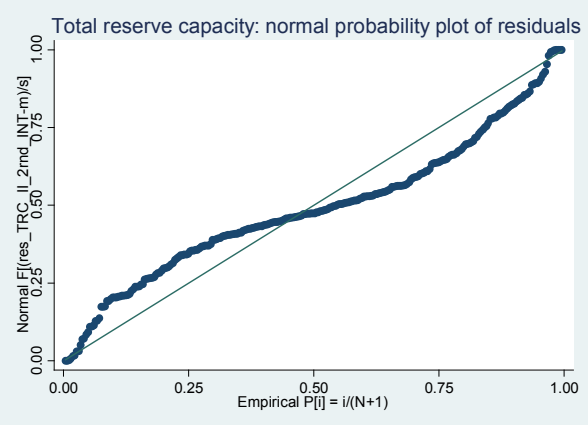

C)

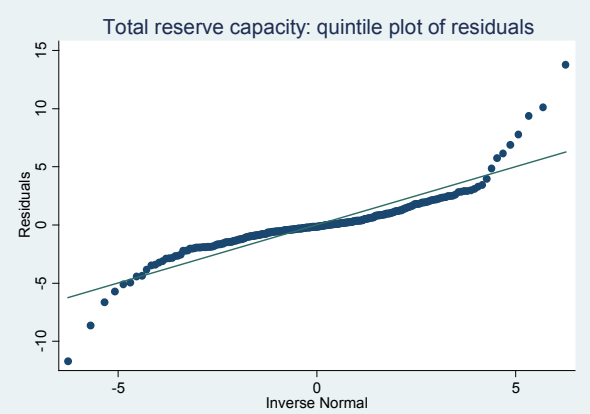

D)

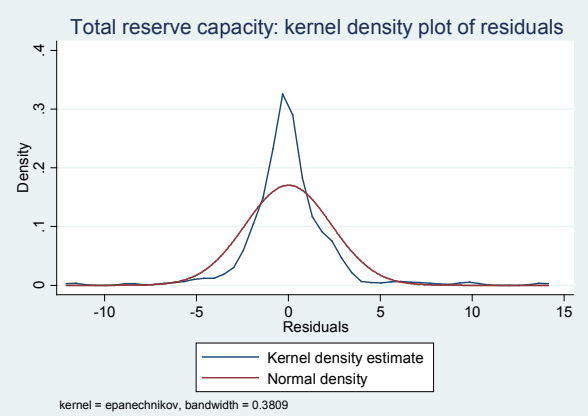

III) ATP-linked OCR

A)

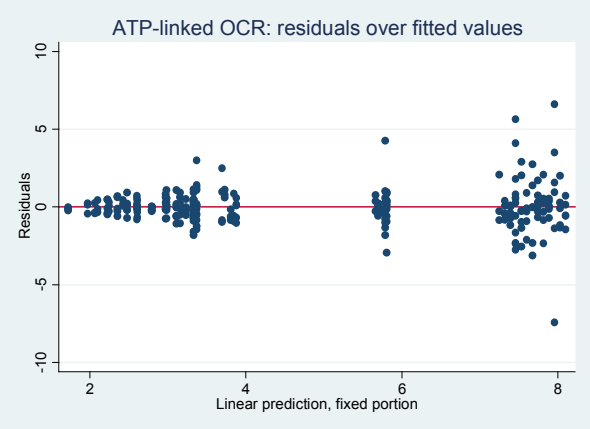

B)

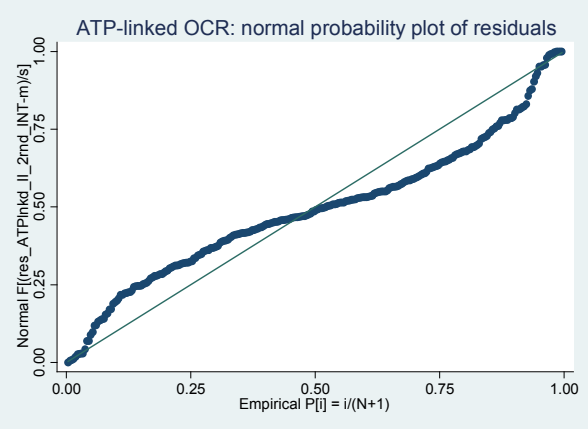

C)

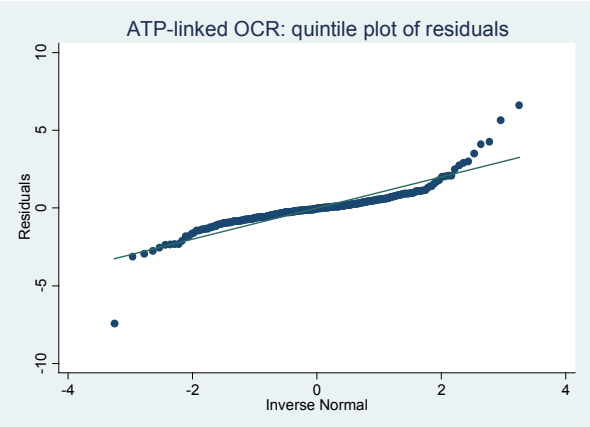

D)

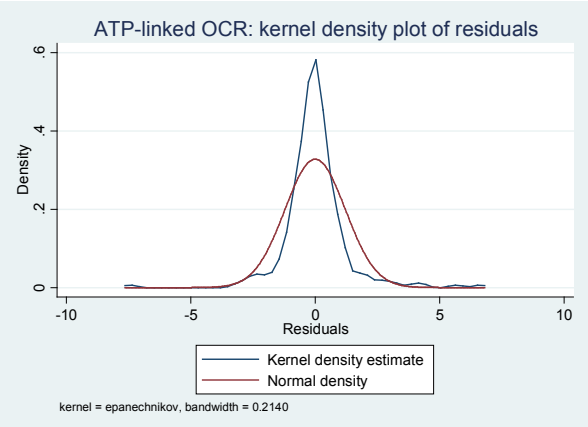

Figure 6. Linear mixed effect model diagnostics of basal OCR I), total reserve capacity II) and ATP-linked OCR III). A) Scatter plot of residuals over the fitted values, B) Standardized normal probability plot of residuals, C) Quantile plot of residuals, D) Kernel density plot of residuals over normal distribution. No significant departure from normality of residuals can be observed in all three linear mixed effect models.

Table 8. Comparisons of basal OCR, total reserve capacity and ATP-linked OCR between pairs of analyzed cell types. The comparison of each pair of different cell type was perform using Wald test.

Cell type			Basal OCR (p-value)	Total Reserve Capacity (p-value)	ATP-linked OCR (p-value)
Normal	vs.	Basal-like	0.8064	0.3283	0.8390
Normal	vs.	Claudin-low	0.7243	0.3011	0.6213
Normal	vs.	Luminal	<0.00001*	0.0010*	0.0002*
Normal	vs.	Her-2	0.0051*	0.0927	0.0848
Basal-like	vs.	Claudin-low	0.8333	0.5042	0.8802
Basal-like	vs.	Luminal	<0.00001*	<0.00001*	0.0001*
Basal-like	vs.	Her-2	0.0112*	0.0467*	0.1555
Claudin-low	vs.	Luminal	<0.00001*	<0.00001*	<0.00001*
Claudin-low	vs.	Her-2	0.0030*	0.0301*	0.0829
Luminal	vs.	Her-2	0.0001*	0.0044*	0.0010*

*statistically significant values at the significance level $p<0.05$

APPENDIX B: STATA CODE

Stata/SE 12 code for linear mixed effect model:

I Variable labeling, recoding and exploratory analysis:

```
label variable mOCR " Mean oxygen consumption rate"
label variable CTYPE "Cell Types"
label values TREATM treatment
label variable TIME "Read out time (min)"
label variable TREATM "Treatment"
label variable CLINE "Cell Lines"
label define Cell_Line 1 "BT-20" 2 "HCC1143" 3 "BT-549" 4 "Hs578T" 5 "MDA-MB 157" 6 "MDA-MB 231" 7 "MCF-7" 8 "BT-474" 9 "ZR-75 1" 10 "CAMA-1" 11 "MDA-MB 361" 12 "SK-BR 3" 13 "MDA-MB 453" 14 "HMEC" 15 "BRL36" 16 "BRL11" 17 "BRL23"
label values CLINE Cell_Line
label define Cell_Type 1 "Basal-like" 2 "Claudine-low" 3 "Luminal" 4 "Her-2" 5 "Normal"
label values CTYPE Cell_Type
label variable EXPDATE "Experiment number (by date)"
label define expdate 1 "exp 1" 2 "exp 2" 3 "exp 3" 4 "exp 4" 5 "exp 5" 6 "exp 6" 7 "exp 7" 8 "exp 8" 9 "exp 9" 10 "exp 10" 11 "exp 11" 12 "exp 12 13 "exp 13" 14 "exp 14" 15 "exp 15"
label values EXPDATE expdate

tabulate CLINE CTYPE
tabulate SUBJECT CLINE

graph box  mOCR, over(CLINE) title("OCR over cell line")
graph box  mOCR, over(CTYPE) title("OCR over cell type")
graph box  mOCR, over(EXPDATE) title("OCR over experiment number")

separate mOCR, by(TREATM)
tabstat mOCR0 , by(CTYPE) statistics (n mean SD min max)
tabstat mOCR1 , by(CTYPE) statistics (n mean SD min max)
tabstat mOCR2 , by(CTYPE) statistics (n mean SD min max)
tabstat mOCR3 , by(CTYPE) statistics (n mean SD min max)
tabstat mOCR4 , by(CTYPE) statistics (n mean SD min max)
```

II linear mixed effect modeling and model diagnostics using two random variables in the model ("cell line" and "experiment number") and the "experiment number" as control variable.

```
xi: xtmixed mOCR ib5.CTYPE EXPDATE || SUBJECT : || EXPDATE:, mle var
predict yhat_mOCR_2rnd, xb
predict res_mOCR_2rnd, r

scatter res_mOCR_2rnd yhat_mOCR_2rnd, yline(0) title("OCR: residuals over fitted values")
pnorm res_mOCR_2rnd, title("OCR: normal probability plot of residuals")
qnorm res_mOCR_2rnd, title("OCR: quintile plot of residuals")
kdensity res_mOCR_2rnd, normal title("OCR: kernel density plot of residuals")


testparm 1.CTYPE
testparm 2.CTYPE
testparm 3.CTYPE
testparm 4.CTYPE
testparm 1.CTYPE 2.CTYPE
testparm 1.CTYPE 3.CTYPE
testparm 1.CTYPE 4.CTYPE
testparm 2.CTYPE 3.CTYPE
testparm 2.CTYPE 4.CTYPE
testparm 3.CTYPE 4.CTYPE


xi: xtmixed BasalOCR ib5.CTYPE EXPDATE|| CLINE : || EXPDATE:, mle var
predict yhat_BOCR_2rnd, xb
predict res_BOCR_2rnd, r

scatter res_BOCR_2rnd yhat_BOCR_2rnd, yline(0) title("Basal OCR: residuals over fitted values")
pnorm res_BOCR_2rnd, title("Basal OCR: normal probability plot of residuals")
qnorm res_BOCR_2rnd, title("Basal OCR: quintile plot of residuals")
kdensity res_BOCR_2rnd, normal title("Basal OCR: kernel density plot of residuals")

testparm 1.CTYPE
testparm 2.CTYPE
testparm 3.CTYPE
testparm 4.CTYPE
testparm 1.CTYPE 2.CTYPE
testparm 1.CTYPE 3.CTYPE
testparm 1.CTYPE 4.CTYPE
testparm 2.CTYPE 3.CTYPE
testparm 2.CTYPE 4.CTYPE
testparm 3.CTYPE 4.CTYPE


xi: xtmixed TotalResOCR ib5.CTYPE EXPDATE|| CLINE : || EXPDATE:, mle var
predict yhat_TotRCap_2rnd, xb
predict res_TotRCap_2rnd, r
```

```
scatter res_TotRCap_2rnd yhat_TotRCap_2rnd, yline(0) title("Total reserve capacity: residuals over fitted values")
pnorm res_TotRCap_2rnd, title(“Total reserve capacity: normal probability plot of residuals”)
qnorm res_TotRCap_2rnd, title(“Total reserve capacity: quintile plot of residuals”)
kdensity res_TotRCap_2rnd, normal title(“Total reserve capacity: kernel density plot of residuals”)

testparm 1.CTYPE
testparm 2.CTYPE
testparm 3.CTYPE
testparm 4.CTYPE
testparm 1.CTYPE 2.CTYPE
testparm 1.CTYPE 3.CTYPE
testparm 1.CTYPE 4.CTYPE
testparm 2.CTYPE 3.CTYPE
testparm 2.CTYPE 4.CTYPE
testparm 3.CTYPE 4.CTYPE

xi: xtmixed ATPLinkedOCR ib5.CTYPE EXPDATE || CLINE : || EXPDATE:, mle var
predict yhat_ATPlnk_2rnd, xb
predict res_ ATPlnk_2rnd, r

scatter res_ATPlnk_2rnd yhat_ATPlnk_2rnd, yline(0) title("ATP-linked OCR: residuals over fitted values")
pnorm res_ATPlnk_2rnd, title(“ATP-linked OCR: normal probability plot of residuals”)
qnorm res_ATPlnk_2rnd, title(“ATP-linked OCR: quintile plot of residuals”)
kdensity res_ATP-linked_2rnd, normal title(“ATP-linked OCR: kernel density plot of residuals”)

testparm 1.CTYPE
testparm 2.CTYPE
testparm 3.CTYPE
testparm 4.CTYPE
testparm 1.CTYPE 2.CTYPE
testparm 1.CTYPE 3.CTYPE
testparm 1.CTYPE 4.CTYPE
testparm 2.CTYPE 3.CTYPE
testparm 2.CTYPE 4.CTYPE
testparm 3.CTYPE 4.CTYPE
```

BIBLIOGRAPHY

1. Donald Voet D, Voet JG. Biochemistry, 3rd edition. John Wiley & Sons, Inc.; 2004.

2. Harold FM. The Vital Force: A Study of Bioenergetics, Chapter 7. Freeman; 1986.

3. Muirhead H, Watskon H. Glycolytic enzymes: from hexose to pyruvate. Curr. Opin. Struct. Biol. 1992; 2: 870-876.

4. Saier MH, Jr. Enzymes in Metabolic Pathways, Chapter 5. Harper and Row; 1987.

5. Hatefi, Y. The mitochondrial electron transport chain and oxidative phosphorylation system. Annu. Rev. Biochem. 1985; 54: 1015-1069.

6. Schultz BE, Chan SI. Structures and proton pumping strategies of mitochondrial respiratory enzymes. Annu. Rev. Biophys. Biomol. Struct. 2001; 30: 23-65.

7. Hinkle PC, Kumar MA, Resetar A, Harris DL. Mechanistic stoichiometry of mitochondrial oxidative phosphorylation. Biochemistry 1991; 20: 3576-3582.

8. Martonosi AN. The Enzymes of Biological Membranes (2nd ed.), Vol 4, Bioenergetics of Electron and Proton Transport. Plenum Press; 1985.

9. Moser CC, Keske JM, Warncke K, Farid RS, Dutton LS. Nature of biological electron transfer. Nature 1992; 355: 796-802.

10. Warburg O. On the origin of cancer cells. Science 1956; 123: 309-314.

11. Pike LS, Smift AL, Nicolev CJ, Ferrick DA, Wu M. Inhibition of fatty acid oxidation by etomoxir impairs NADPH production and increases reactive oxygen species resulting in ATP depletion and cell death in human glioblastoma cells. Biochimica et. Biophysica Acta 2011; 1807: 726-734.

12. DeBerardinis RJ, Lum JJ, Hatzivassiliou G, Thompson CB. The biology of cancer: metabolic reprogramming fuels cell growth and proliferation. Cell Metab. 2008; 7: 11-20.

13. Vander Heiden MG, Cantley LC, Thompson CB. Understanding the Warburg effect: the metabolic requirements of cell proliferation. Science 2009; 324: 1029-1033.

14. Debarardinis RJ, Sayed N, Ditsworth D, Thompson CB. Brick by brick: methabolism and tumor cell growth. Curr. Opin. Genet. Dev. 2008; 18:54-61.

15. Dang CV, Rethinking the Warburg effect with Myc micromanaging glutamine methabolims. Cencer Res. 2010; 70: 859-862.

16. Wu M, Neilson A, Swift AL, Moran R, Tamagnine J, Parslow D, Armistead S, Lemire K, Orrell J, Teich J, Chomicz S, Ferrick DA. Mutliparameter metabolic analysis reveals a close link between attenuated mitochondrial bioenergetics function and enhanced glycolysis dependency in human tumor cells. Am.J.Physiol Cell Physiol 2007; 292: C125-C136.

17. Hill BG, Dranka BP, Zou L, Chatham JC, Darley-Usmar VM. Importance of bioenergetic reserve capacity in response to cardiomyocyte stress induced by 4-hydroxynonenal. Biochem. J. 2009; 424:99-107.

18. Randle PJ. Regulatory interactions between lipids and carbohydrates: the glucose fatty acid cycle after 35 years, Diabetes/Metab. Rev 1998; 14: 263-283,

19. Harris DA, Das AM. Control of mitochondrial ATP synthesis in the heart. Biochem. J. 1991; 280: 561-573.

20. Prat A, Parker JS, Karginova O, Fan C, Livasy C, Herschekowitz JI, Perou CM. Phenotypic and molecular characterization of the claudin-low intrinsic subtype of breast cancer. Breast Cancer Research 2010; 12:R68

21. Andersen PK, Skovgaard LT. Regression with Linear Predictors, Springer Science+Business Media, LLC; 2011

22. Twisk WR. Applied Longitudinal Data Anlysis for Epidemiology, A Practical Guide, Cambridge University Press; 2003

23. Fitzmaurice GM, Laird NM, Ware JH. Applied Longitudinal Analysis, Wiley Series in Probability and Statistics. Wiley-Interscience; 2004.

24. Bain LJ, Engelhard M. Introduction to probability and mathematical statistics. Duxbury; 1992.

25. Ferrick DA, Neilson A, Beeson C. Advances is measuring cellular bioenergetics using extracellular flux. Drug Discovery Today, 2008; 13: 268-274.